Molecular Therapy
Methods & Clinical Development
Original Article

Genetic alteration of SJ293TS cells and modification of serum-free media enhances lentiviral vector production

Matthew Bauler,[1] Francesca Ferrara,[1] Brandon Lowe,[1] Jordan A. Beard,[1] Chris Wincek,[1] Matthew M. Wielgosz,[1] Jeoungeun J. Park,[2] Na Shang,[2] Saikat Nandy,[3] Cai Li,[3] Deanna M. Langfitt,[4] Sheng Zhou,[2] and Robert E. Throm[1]

[1]Vector Development and Production Laboratory, St Jude Children's Research Hospital, Memphis, TN 38105, USA; [2]Experimental Cell Therapeutics Lab, St Jude Children's Research Hospital, Memphis, TN 38105, USA; [3]Biostatistics, St Jude Children's Research Hospital, Memphis, TN 38105, USA; [4]Bone Marrow Transplant and Cell Therapy, St Jude Children's Research Hospital, Memphis, TN 38105, USA

Successful cell and gene therapy clinical trials have resulted in the US Food and Drug Administration and European Medicines Agency approving their use for treatment of patients with certain types of cancers and monogenetic diseases. These novel therapies, which rely heavily on lentiviral vectors to deliver therapeutic transgenes to patient cells, have driven additional investigations, increasing demand for both pre-clinical and current Good Manufacturing Practices-grade viral vectors. To better support novel studies by improving current production methods, we report the development of a genetically modified HEK293T-based cell line that is null for expression of both Protein Kinase R and Beta-2 microglobulin and grows in suspension using serum-free media, SJ293TS-DPB. Absence of Protein Kinase R increased anti-sense lentiviral vector titers by more than 7-fold, while absence of Beta-2 microglobulin, a key component of major histocompatibility complex class I molecules, has been reported to reduce the immunogenicity of lentiviral particles. Furthermore, we describe an improved methodology for culturing SJ293TS-DPB that facilitates expansion, reduces handling, and increases titers by 2-fold compared with previous methods. SJ293TS-DPB stably produced lentiviral vectors for over 4 months and generated lentiviral vectors that efficiently transduce healthy human donor T cells and CD34$^+$ hematopoietic stem cells.

INTRODUCTION

Lentiviral vectors (LVs), based on the human immunodeficiency virus-1 (HIV), are commonly used to stably transfer genetic cargo into cells for both basic research and therapeutic purposes.[1,2] LVs are excellent choices to support cell and gene therapy studies due to the ability to achieve relatively high titers (>10^9 transducing units [TUs] per mL), transduce both dividing and non-dividing cells, be pseudotyped with envelope proteins from other viruses, package payloads up to 9 kb, stably integrate into the genome of target cells, and demonstrate a safer pattern of integration compared with simple gamma-retroviruses.[3–7] Currently, LVs are the vector of choice for hundreds of ongoing Phase I/II clinical trials, and eight drug products have been approved by the US Food and Drug Administration (FDA) and European Medicines Agency (EMA) with more approvals expected soon.[8,9] In 2019, former FDA Commissioner Scott Gottlieb predicted that by 2025, the agency would be approving 10 to 20 new gene and cell therapy products each year.[10] Historically, production of LVs has mostly depended upon transient transfection of adherent HEK293T cells grown in fetal bovine serum-containing media using multiple plastic vessels.[3,4,11] However, this approach does not effectively support large-scale LV production under current Good Manufacturing Practices (cGMP) due to the labor-intensive nature of the process, cost, variability of serum and inability to scale-up. To alleviate this bottleneck, several investigators, including us with our own SJ293TS cell line, have reported the successful use of fixed bed bioreactors, stable producer cell lines, and HEK293T cells grown in suspension using serum-free media (SFM) to facilitate cGMP LV production.[4,12–18] Despite these advances, further improvements are needed, especially for LV containing expression cassettes in the reverse orientation.

Clinically appropriate LVs are self-inactivating because the enhancer and promoter elements within the HIV 3′ U3 domain of the viral long terminal repeat (LTR) are deleted.[1,19] This prevents mobilization of the vector after transduction and minimizes effects on neighboring genes after integration, thereby reducing deleterious insertion events and improving overall safety. Thus, self-inactivating LVs are dependent upon internal promoters for transgene expression. In most cases, expression cassettes are transcribed in the same direction as the vector genome during production (sense LVs). However, in some instances, as with therapeutic β- or γ-globin expressing vectors, placing the expression cassette in the reverse orientation relative to viral genomic transcription is necessary to prevent splicing and maintain regulatory elements.[20–23] Other examples include using a bidirectional promoter for the expression of multiple open reading frames (ORFs) or including a

Received 9 January 2024; accepted 17 May 2024;
https://doi.org/10.1016/j.omtm.2024.101270.

Correspondence: Robert E. Throm, St Jude Vector Laboratory, St Jude Children's Research Hospital, 262 Danny Thomas Place, Memphis, TN 38105, USA.
E-mail: robert.throm@stjude.org

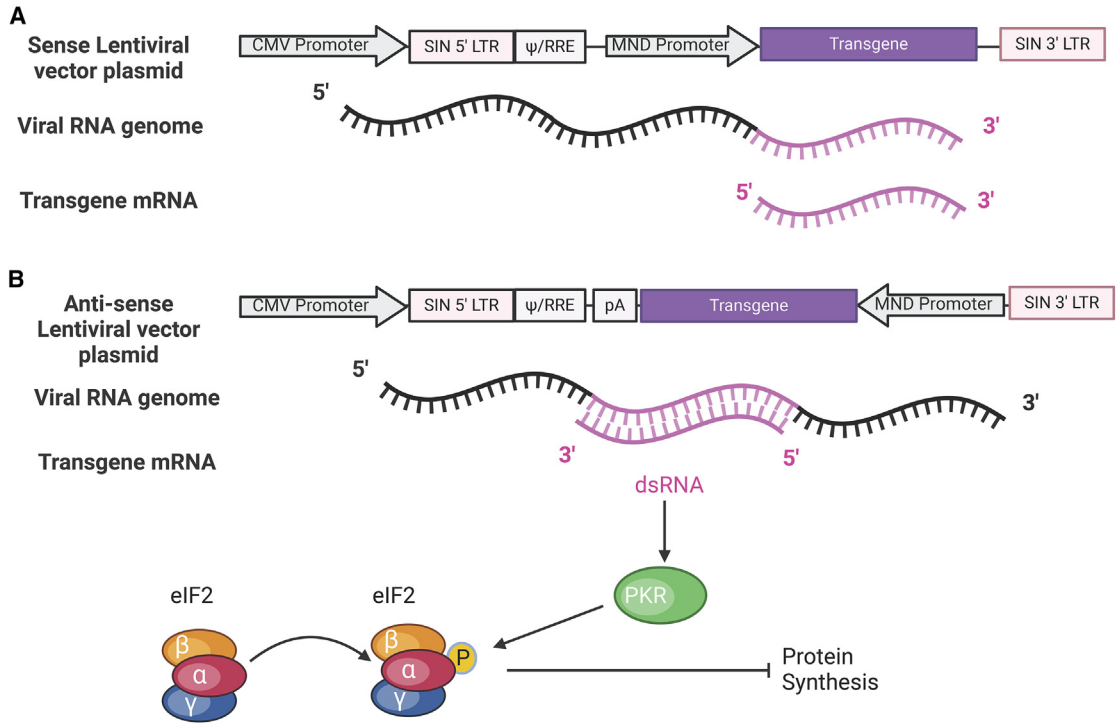

Figure 1. RNA transcripts formed during production of sense and anti-sense lentiviral vectors

(A) Sense lentiviral vectors with an internal promoter yield RNA transcripts that are noncomplementary. (B) Anti-sense lentiviral vectors with an internal promoter form RNA transcripts that are complementary. Binding of dsRNA by PKR leads to activation of PKR and phosphorylation of the eIF2 a subunit leading to inhibition of protein synthesis. Reduced protein synthesis leads to significantly lower vector production. Created with BioRender.com.

strong dedicated polyA signal to benefit transgene expression.[24–26] Such LVs are referred to as anti-sense LVs in this report. Because transcription of the vector genome and transgene occurs simultaneously in opposite directions during vector production, the resulting RNA transcripts are complementary and can lead to the formation of double-stranded RNA (dsRNA) (Figure 1), resulting in poor titers.

The presence of dsRNA is commonly associated with viral infections within cells. In response, vertebrates have evolved overlapping mechanisms to detect dsRNA as part of the cellular innate immune pathway. These dsRNA sensors include Protein Kinase R (PKR), 2′-5′ oligoadenylate synthetases (2′-5′ OAS1, OAS2, OAS3, and OASL), Toll-like receptor family members (TLR-3, 7, and 8), members of the RIG-I-like receptors (RIG-1, MDA5, and LGP2) and the NACHT, LRR, and FIIND CARD domain and PYD domain-containing protein 1 (NLRP1).[27–29] Activation of the innate immune system can lead to a type I interferon response, inhibition of protein synthesis, RNA degradation, and apoptosis. The production of LV relies almost exclusively on the usage of HEK293T cells. Although these cells do not have a fully functioning innate immune system, PKR is expressed in HEK293T cells, and its loss/inhibition increases anti-sense LV titers.[30,31] While other investigators have blocked or knocked out PKR in HEK293T cells, these cell lines are not readily amenable to large-scale clinical-grade LV production.[26,32] Previously, we developed SJ293TS cells grown in suspension using SFM to support clinical-grade LV production.[13] Here, we report a next generation cell line that does not express PKR and completely restores anti-sense LV titers to levels comparable with forward-orientation LVs. We also knocked out Beta-2 microglobulin (B2M) to prevent carryover of the major histocompatibility complex class I molecules (MHC-I) from the surface of producer cells to viral particle envelopes during the budding process. As reported by Milani et al., loss of B2M in producer cells resulted in MHC-I free LV particles which were less immunogenetic in *in vitro* assays and may be better suited for use *in vivo* than MHC-containing LV particles.[33] This new PRK-null, B2M-null cell line is referred to as SJ293TS-Delta PKR-B2M (SJ293TS-DPB). Additionally, by optimizing culture conditions using a nutrient-dense media as a supplement, we significantly improved LV titers 2-fold compared with our previous method while also reducing the amount of labor required to maintain the cells, making this a preferred system in a cGMP environment. Finally, we demonstrate that LVs derived from this new cell line are efficient at transducing primary human cells such as T cells and $CD34^+$ cells.

RESULTS

Knocking out PKR and B2M in SJ293TS improves LV titers

Early-passage SJ293TS cells were transduced with lentivirus-based virus-like particles packaging Cas9 and single guide RNA (sgRNA)

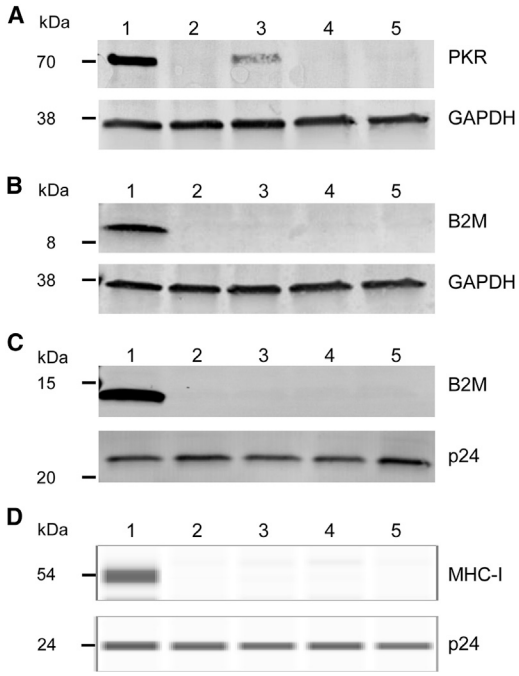

Figure 2. Western blot analysis of clones

Whole cell lysates from (1) SJ293TS, clones (2) 39G4, (3) 4E3, (4) 31G12, and (5) 34D5 were assayed for expression of either (A) PKR or (B) B2M. Expression of GAPDH was used as a loading control, and approximate migration of protein standards are indicated to the left of each blot. In (C) and (D), equal amounts of purified viral particles, as determined by equal p24 loading, derived from (1) SJ293TS, clones (2) 39G4, (3) 4E3, (4) 31G12, and (5) 34D5 were assayed for presence of B2M or MHC-I, respectively.

(Cas9-VLP) to disrupt the ORF of both *EIF2AK2* and *B2M*, which encode the proteins PKR and B2M, respectively, by creating small insertions or deletions (INDELs) within the cellular genome. Four Cas9-VLP preparations were made; two targeting *EIF2AK2* within exons 3 and 4 and two targeting *B2M* within exons 1 and 2 (Table S1). We chose two sites per target such that concurrent cutting could result in complete deletion of the intervening sequence between the two exons of 4,092 base pairs (bp) in *EIF2AK2* and 891 bp in *B2M*, respectively, to increase disruption of the ORF. SJ293TS cells were transduced with both Cas9-VLPs targeting *EIF2AK2*. Forty-eight hours later, the same cells were then transduced with two preparations of Cas9-VLP targeting *B2M*. After another 48 h, individual clones were isolated by limiting dilution and expanded. At the same time, we used targeted deep sequencing using next generation sequencing (NGS) to evaluate editing within the bulk population (Table S2). For *EIF2AK2*, INDEL formation was detected in 32.2% of exon 3 reads and 53.3% of exon 4 reads, while INDEL formation was detected in 77.1% of *B2M* exon 1 reads and 24.8% of *B2M* exon 2 reads. Targeted deep sequencing also detected large deletions of the intervening sequence between exons of both genes suggesting simultaneous editing occurred. Although these large deletions resulted in sequence reads of varying length and sequence, approximately 20% (18.5% and 19.3% for *EIF2AK2* and *B2M*, respectively) were exactly as predicted based on Cas9 cutting between the third and fourth nucleotide of the protospacer upstream of the PAM sequence. Thus, we estimated that at least 41% of cells contained knockout of both genes.

We used anti-sense LV production as a screen for loss of PKR in individual clones. We screened 45 individual clones using an anti-sense LV, SJL21-MND-GFP, and compared titers with LV preparations generated from the parent cell line, SJ293TS. We included an LV with an expression cassette in the forward orientation, SJL12-MND-GFP, as a control. Both LVs expressed a GFP reporter, and transfections were performed at 5-mL scale and not diluted post-transfection. As expected, the SJ293TS-produced anti-sense LV had a 4-fold lower titer than the sense LV (0.8×10^8 vs. 3.1×10^8 TUs/mL). While most clones produced SJL12-MND-GFP similarly to the parent, eight clones produced anti-sense LV titers >3-fold higher (range 3.1–5.6-fold) compared with the parental cell line, suggesting at least partial loss of PKR in these clones (Figure S1). These clones were also assayed for loss of B2M expression by cell surface staining and flow cytometry (Figure S2). Of these top eight anti-sense LV producing clones, five were negative and three were positive for B2M expression. The three B2M-positive clones and one B2M-negative clone, 3A7, which was highly aggregate in culture, were excluded from further study. NGS data from the four remaining clones indicated the presence of INDELs within all copies of the *EIF2AK2* and *B2M* ORF except for possibly one *EIF2AK2* allele in clone 4E3, which appeared intact (data not shown). Generally, these INDELs resulted in the insertion of a stop codon or alternate ORF creating missense or truncated protein. Western blot analysis of whole cell lysates and purified viral particles confirmed loss of PKR and B2M expression in these clones, except for clone 4E3, which retained partial PKR expression (Figures 2A–2C). Consistent with the loss of B2M, MHC-I could not be detected on the surface of B2M null clones or in purified viral particles (Figures 2D and S3). Despite partial retention of PKR expression by clone 4E3, we continued to evaluate it given that initial anti-sense LV titers were >3-fold higher than the parent suggesting partial knockdown of PKR is sufficient to overcome low anti-sense LV titers. Next, to identify a clone that was readily transfected and could consistently produce high titers of the more commonly used sense LV, we repeatedly produced SJL12-MND-GFP from each clone and compared the transfection efficiency and resulting titers to the parent, SJ293TS (Figure 3). While there were no statistically significant differences in titer or transfection efficiency, the mean titer and transfection efficiency of clones 31G12 and 34D5 tended to be slightly lower than the parental cell line. In contrast, the mean titer and transfection efficiency of clones 39G4 and 4E3 were slightly higher than the parental cell line, suggesting they were not inferior to SJ293TS cells. Thus, we narrowed our focus further by continuing to study only the highest-performing clones, 39G4 and 4E3.

To evaluate the clones more rigorously, SJ293TS cells, along with clones 4E3 and 39G4, were continuously passaged for 4 months by three independent operators and were periodically transfected to

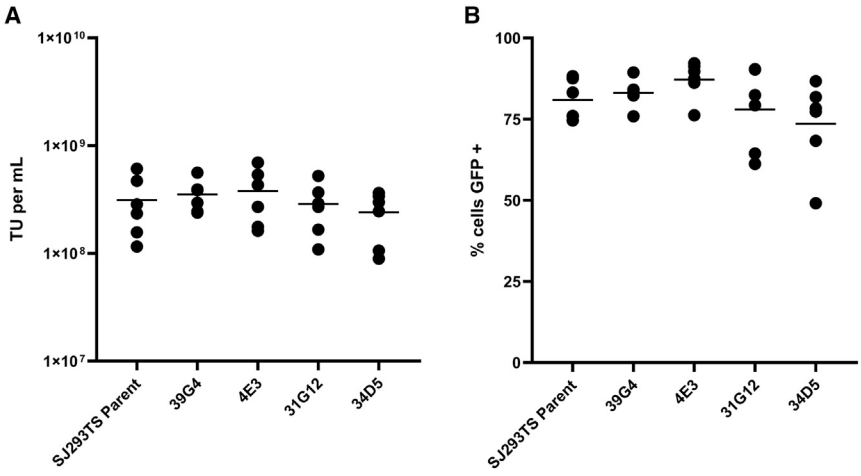

Figure 3. Comparison of top clones

Top four clones along with the parental cell line, SJ293TS, were used to produce a GFP-expressing lentiviral vector, SJL12-MND-GFP. (A) Replicate titers and mean (bar) are shown. (B) Transfection efficiency for each replicate and mean (bar) are shown. $N = 6$.

produce two simple GFP-expressing sense and anti-sense LV vectors, SJL12-MND-GFP and SJL21-MND-GFP, respectively, and one clinically relevant anti-B7-H3 chimeric antigen receptor (CAR) expressing LV, SJL651. To reduce potential variability inherent with titration, vector preparations, upon harvest, were stored at −80°C until completion of the study, and subsequently titered at the same time (Figure 4). Although some variability was evident between time points, there were no significant decreases in titer from any cell line regardless of vector produced. All three cell lines produced similar titers of SJL12-MND-GFP on average. As expected, anti-sense LV titers produced by both clones were significantly higher than those produced by SJ293TS ($p < 1 \times 10^{-7}$) (Figure 4B). Clones 39G4 and 4E3 produced, on average, 7.6-fold and 4.9-fold more anti-sense LV TUs, respectively, than SJ293TS cells. Interestingly, the mean anti-sense LV titer derived from clone 39G4 was also significantly higher than the mean anti-sense LV titer produced by clone 4E3 by 1.6-fold ($p = 0.002$) likely due to clone 4E3's partial PKR expression. Last, statistical analysis comparing the mean titers of SJL651 generated from each cell line indicated that clone 39G4 produced significantly more TUs than both the parental cell line and clone 4E3 ($p = 0.004$ and 0.003, respectively). Thus, clone 39G4 was chosen for further study and designated as SJ293TS-DPB.

Addition of LV-MAX media to FreeStyle 293 expression media improves titers and reduces handling

Next, we characterized SJ293TS-DPB growth in culture. Growth curves comparing SJ293TS and SJ293TS-DPB cultured in FreeStyle 293 Expression medium (FreeStyle) were similar (Figure S4) with cell density peaking around 3×10^6 per mL before declining. This means that at the time of transfection, when cells are seeded at 2×10^6 per mL, the media is unlikely to fully support the cells during 48 h of vector production. Thus, we reasoned that an SFM capable of sustaining a higher cell density may allow cells to be more productive after transfection by providing a more nutrient-rich environment. To test this, we replaced our current media, FreeStyle, with LV-MAX, an SFM reported to support HEK293 cell densities up to 10^7 cells per mL. With clinical-grade large-scale production in mind, we supplemented FreeStyle with various amounts of LV-MAX to reduce costs, since LV-MAX costs more than twice as much as FreeStyle. To this end, SJ293TS-DPB cells were adapted to grow in LV-MAX alone (100%) or FreeStyle supplemented with 10%, 20%, 30%, or 50% LV-MAX. SJ293TS-DPB cells were thawed directly into the various media formulations and cultured for 5 weeks to ensure the cells had fully adapted before testing was performed. Typically, subculturing cells involves pelleting and suspending cells in 100% fresh FreeStyle. However, this manipulation is time-consuming, increases the risk of contamination, and is impractical for volumes larger than 1 L. Thus, we assessed whether SJ293TS-DPB cells, regardless of media formulation, could maintain high-titer LV production when passaged and prepared for transfection only by dilution with fresh media. For passaging, all cell cultures were maintained at a similar cell density, which was typically $\sim 3 \times 10^6$ cells per mL before diluting to 4 to 5×10^5 cells per mL with fresh media. Since cell cultures were seeded at 2×10^6 per mL for immediate transfection (referred to as "same day" transfections), they typically contained around 60%–80% conditioned media. We also seeded cells at an initial lower cell density of 1×10^6 per mL so that the conditioned media content was reduced by half. We then allowed these cells to grow for 24 h to reach $\sim 2 \times 10^6$ per mL before proceeding with transfection (referred to as "next day" transfections). Prior to this experiment, we verified that SJ293TS-DPB maintained similar doubling times, regardless of media formulation, so that 24 h after seeding, the cultures would reach the desired cell density (data not shown). As a control for these experiments, we included SJ293TS-DPB cells that were maintained and prepared for transfection as described above by suspending cell pellets in completely fresh FreeStyle. Regardless of the day of transfection, the resulting titers showed the same trend for each group (Figure 5). Transfecting cells in 100% fresh FreeStyle media (control) led to higher titers compared with transfection in cultures containing conditioned FreeStyle media, although only next day transfections produced titers that were statistically different ($p = 6.7 \times 10^{-5}$). Supplementing FreeStyle media with 10%, 20%, or 30% LV-MAX also resulted in increased titers with 30% LV-MAX achieving the highest titer relative to the control group (2.4- and 2.7-fold increases for next day and same day transfections, respectively). Interestingly, despite having higher transfection rates, cells cultured in 50% LV-MAX had only modestly improved titers of 1.2- to 1.5-fold vs. the control group (Figures 5 and S5). Similarly, cells cultured in 100% LV-MAX also had higher transfection efficiency compared with the control group, but titers were reduced by 3-fold. These results suggest

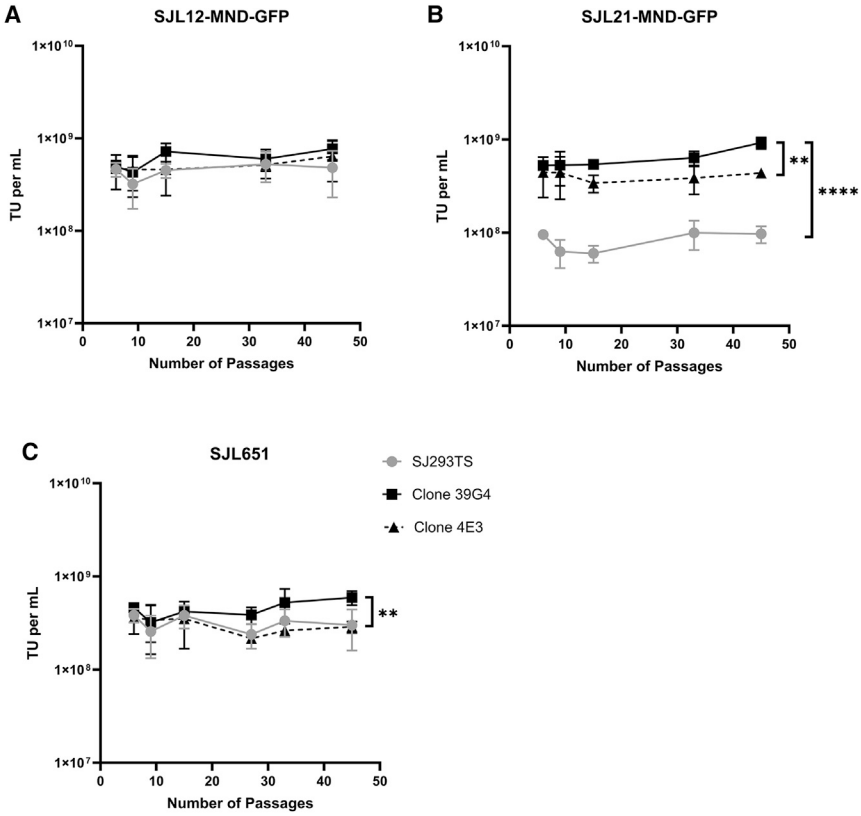

Figure 4. Production of lentiviral vectors over time

SJ293TS (gray circles), Clone 39G4 (black square), and Clone 4E3 (black triangle) were continuously passaged for 4 months and periodically used to produce (A) SJL12-MND-GFP, (B) SJL21-MND-GFP, or (C) SJL651. All data points were performed in either duplicate or triplicate, and significance is based on the average of all data points for the relevant cell line and vector. $^{**}p \leq 0.01$, $^{****}p \leq 0.0001$.

that concentrations ≥50% LV-MAX have a negative effect on LV production. Although cells cultured in 30% LV-MAX had the highest titers, titers from cells cultured in 20% LV-MAX were not significantly different (same day $p = 0.47$, next day $p = 1$). In contrast, next day titers from cells cultured in 20% LV-MAX were significantly higher than titers from cells grown in 10% LV-MAX ($p = 0.014$). For this reason and to reduce costs while significantly increasing titers, all succeeding studies were performed with SJ293TS-DPB cells cultured in FreeStyle with 20% LV-MAX. Furthermore, the addition of LV-MAX had no impact on downstream purification as yields from 1-L vector preparations, 54% ± 12%, $N = 38$, were similar to those previously reported (Table S3).[13]

Optimizing SJ293TS-DPB cell density and growth phase for lentiviral vector production

Follow-up experiments characterizing the growth of SJ293TS-DPB cells in FreeStyle with 20% LV-MAX showed that cell densities could reach ~5×10^6 per mL with viability >98% before declining (Figure S4). Since FreeStyle with 20% LV-MAX could support higher cell densities, we examined if increasing cell density at the time of transfection would lead to increased titers. In this experiment, SJ293TS-DPB cells were expanded to 4.8×10^6 per mL before seeding for transfection at our standard cell density of 2×10^6 per mL and at higher cell densities of 3 and 4×10^6 per mL. Although the amount of DNA and PEI per million cells was kept constant, there was no increase in TU per mL and transfection efficiency decreased with increasing cell density (Figure S6). Next, we examined if the phase of cellular growth would affect LV production. To test this, three separate cultures of SJ293TS-DPB cells were grown to cell densities of either 3×10^6, 4×10^6, or 5.4×10^6 per mL. Based on the growth curve in Figure S4, we considered these cultures to be in log, late-log, or stationary phase, respectively. Each culture was used to seed shaker flasks at either 2×10^6 cells per mL for same day transfection or 1×10^6 cells per mL for next day transfection (Figure S7). Regardless of day of transfection, cells in log phase produced significantly more TU than cells in stationary phase ($p < 0.05$). Cells in late-log phase also produced significantly more TU than cells in stationary phase but only when transfected the next day ($p < 0.05$). Regardless of significance, there was a clear trend where cells in log phase produced more TUs than cells in stationary phase. Thus, for future vector production, cells were not expanded beyond 4×10^6 per mL to keep them in either log or late-log phase.

Post-transfection handling

As previously reported, vector preparations scheduled for downstream processing are diluted 24 h post-transfection with an equal volume of FreeStyle media containing Benzonase to degrade residual plasmid DNA and limit the cytotoxicity associated with transfection. Here, we examined if diluting the cells at an earlier time point, 6-h post-transfection, would provide a boost to titers over the previously used time point of 24 h. In addition, we also compared the type of media used to dilute the cells, FreeStyle only or FreeStyle with 20% LV-MAX media. In this experiment, cells cultured in FreeStyle with 20% LV-MAX were transfected and either not diluted (control), diluted with FreeStyle only, or FreeStyle with 20% LV-MAX at 6-h or 24-h post-transfection (Figure S8). Generally, diluting cells 6-h post-transfection using FreeStyle provided the greatest benefit (average 19% increase in TUs/mL, range 8%–31%). Dilution at 6 h with FreeStyle with 20% LV-MAX media also increased titers, but the benefit was slightly lower (average 14% increase in TU/mL, range 8%–22%). Diluting cultures 24 h post-transfection with FreeStyle had less impact on titers (average 8% increase in TUs/mL, range 3%–15%), while FreeStyle with 20% LV-MAX had no effect (average 0% increase in TUs/mL, range −4% to 6%). Although the increases in titers did not reach

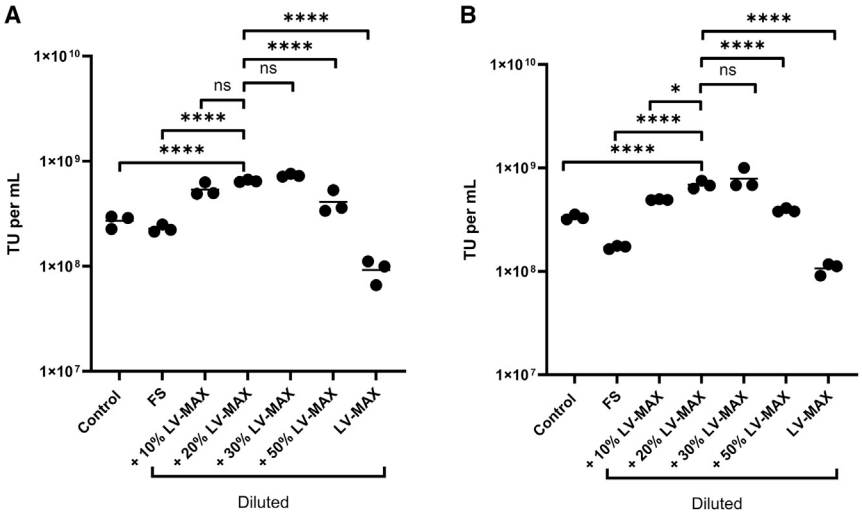

Figure 5. Titers from SJ293TS-DPB grown in various media

SJ293TS-DPB was grown in FreeStyle 293 Expression media (FS) alone, supplemented with various amounts of LV-MAX media or LV-MAX media only. All cultures were maintained by dilution of culture stocks with fresh media as indicated except for "Control" in which the cells were pelleted and suspended in fresh media only. Cells were seeded at a cell density of either (A) 2×10^6 per mL and transfected immediately or (B) 1×10^6 per mL and transfected 24 h later with SJL12-MND-GFP. All transfections were performed in triplicate. ns = not significant, $^*p = 0.05$, $^{****}p \leq 0.0001$.

statistical significance, we chose to dilute vector preparations with FreeStyle media 6-h post transfection for future vector production.

Primary cell transduction

To confirm that LV derived from SJ293TS-DPB could efficiently transduce primary cells commonly used in cell and gene therapies, namely T cells and CD34$^+$ hematopoietic stem cells (HSCs), we produced clinically relevant LVs from both SJ293TS cells cultured in FreeStyle and SJ293TS-DPB cells grown in FreeStyle with 20% LV-MAX according to the optimized procedures described above. For T cell studies, we produced the LV, SJL643, which expresses CD20 and a CAR targeting CD123, and for CD34$^+$ HSC transductions, we produced the LV, CL40i4r-EF1a-hgcOPT, which expresses a codon-optimized human common gamma chain. These vector preparations were purified and concentrated using a scaled-down process comparable to our cGMP downstream process, which includes anion-exchange followed by buffer exchange as described in materials and methods. SJ293TS-DPB cells produced 1.8- and 1.6-fold more TUs of SJL643 and CL40i4r-EF1a-hgcOPT, respectively, than did SJ293TS cells with a similar increase in p24 (Table 1).

T cells from three healthy donors were transduced at three multiplicities of infection (MOIs) with SJL643 produced from both parent and SJ293TS-DPB cell lines. After 7 days, T cells were analyzed for vector copy number (VCN), CAR expression, and CD4/CD8 ratios (Figure 6). The results illustrate that LVs derived from SJ293TS-DPB efficiently transduce human CD4$^+$ and CD8$^+$ T cells leading to high levels of CAR expression even at low MOIs and are not inferior to LVs derived from SJ293TS cells.

Next, human CD34$^+$ HSCs from three healthy donors were transduced with CL40i4r-EF1a-hgcOPT made from both cell lines at an MOI of 50. We determined the VCN for cells maintained in bulk liquid culture 7 days post-transduction (bulk), long-term HSC, defined as CD34$^+$, CD38$^-$, CD90$^+$, CD45RA$^-$, 4 days post-transduction (LT-HSC), and pooled colony-forming unit cells 12 days post-transduction (CFU-C). VCN in CD34$^+$ HSC bulk cultures, LT-HSC and pooled CFU-C were similar (Figure 7A). In addition, the number and type of CFU-C that grew in Methocult were also similar (Figure 7B). Thus, we conclude that SJ293TS-DPB cells grown in FreeStyle with 20% LV-MAX produce LV with higher titers than SJ293TS cells and are capable of efficiently transducing primary human T cells and CD34$^+$ HSCs.

DISCUSSION

Presently, the FDA and EMA have approved a total of eight cell therapies using LVs.[8,9] In addition, hundreds of early-stage gene and cell therapy clinical trials also rely upon LVs for therapeutic transgene delivery. Recently, a review of the field of cell and gene therapy reported that LVs are employed in 26% of all known viral gene therapies, reinforcing the significant role held by this vector system and demands placed on manufacturers to support these studies.[9] Thus, the production of LVs is a key step in drug discovery and availability, and efforts to improve LV production are needed to reduce costs and keep pace with demand. Historically, cGMP production methods have been laborious, inconsistent, and difficult to scale up using adherent cells grown in the presence of fetal bovine serum.[2–4,11] Consequently, manufacturers have scaled out production using multiple plastic vessels, increasing both consumable and labor costs as well as production timelines. In recent years, reports describing the use of stable producer cell lines, fixed bed bioreactors, and suspension cells using SFM designed for use in stirred tank bioreactors or rocking platforms have helped alleviate many difficulties in cGMP LV manufacturing.[4,12–18] Vector design itself has concurrently improved with the increased use of anti-sense-oriented constructs.[20–26] Hu et al. reported that anti-sense LVs provide higher levels of expression on a per copy basis and demonstrate lower rates of mobilization than sense-LV.[26] Since integrations are inherently mutagenic, anti-sense LVs may offer safety advantages compared with sense LVs by providing similar levels of expression at lower VCN.[34] Both scale-up efficiency/cost and LV expression levels are important considerations for therapeutic LVs. To date, there is a lack of development of cGMP manufacturing of anti-sense LV, rendering a valuable gene therapy tool difficult to utilize clinically. While other investigators have made PKR knockout cell lines, these lines are adherent and serum-dependent.[26,30,32]

Table 1. Production, purification, and characterization of clinically relevant lentiviral vectors

	SJ293TS				SJ293TS-DPB			
Vector Prep	TU/mL	p24 mg/mL	TU yield	p24 yield	TU/mL	p24 mg/mL	TU yield	p24 yield
SJL643 uncon	1.1×10^8	3.2	N/A	N/A	2.0×10^8	5.2	N/A	N/A
SJL643 purified	1.8×10^9	29	33%	30%	3.9×10^9	78	40%	30%
hgcOPT uncon	1.6×10^8	3.7	N/A	N/A	2.5×10^8	5.9	N/A	N/A
hgcOPT purified	3.8×10^9	72	48%	39%	4.9×10^9	125	45%	43%

N/A, not applicable; uncon, unconcentrated raw supernatant.
purified, final 0.22-μm filtered material after anion-exchange and buffer-exchange.

Here, we describe a PKR, B2M double-knockout 293T suspension cell line, SJ293TS-DPB, capable of stably providing high titer sense and anti-sense LV vector preparations while growing in suspension using SFM. Loss of PKR in SJ293TS-DPB cells significantly improved anti-sense LV titers >7-fold higher compared with the parental cell line, SJ293TS. In addition, SJ293TS-DPB cells also tended to produce more sense LVs than PKR-expressing SJ293TS cells. This increase does not seem to be unique to SJ293TS-DPB cells, as other investigators who have knocked out expression of PKR in 293T cells also report increases in sense LV titers,[26,30,32] although the mechanism for this improvement is not clear. Hu et al. suggested that low levels of anti-sense mRNA may be formed by the activity of weak promoters within the HIV-1 sequences.[26] Similarly, anti-sense mRNA may be formed by unexpected bidirectional transcription from internal promoters used for transgene expression.[35] Alternatively, the TAR RNA stem loop, which is formed at the very 5′ end of all LV genomes, can be recognized as a dsRNA by PKR. While high levels of TAR have been reported to inhibit PKR,[36–39] cells with low levels of vector plasmid uptake may produce levels of TAR that are unable to inhibit PKR. This may be particularly true for large complex LVs such that the absence of PKR may be favorable during vector production.

To enhance the production of clinical-grade LVs, we simplified and improved the expansion of cells for LV production by supplementing FreeStyle with LV-MAX. Our data show that when cells are serially passaged by dilution with fresh FreeStyle, titers decline compared with cells undergoing a complete media exchange. A complete media exchange is costly, time-consuming, and laborious, particularly in a cGMP setting where volumes can exceed hundreds of liters. By supplementing FreeStyle with LV-MAX, we serially passaged cells by dilution while improving titers 2- to 3-fold, thereby eliminating the need for a complete media exchange.

Our data demonstrate that LVs produced using our cell line and optimized culture conditions transduce primary cells as well or better than LVs produced from the parental cell line. Milani et al. suggested that LV particles lacking B2M may be better suited for *in vivo* usage,[33] as they found that B2Ms containing viral particles were more immunogenic than viral particles lacking B2M. In principle, B2M-negative LVs should reduce the likelihood that recently transduced cells would be cleared by the immune system. Current CAR-T cell immunotherapies are manufactured *ex vivo*, which is a time-consuming task that is highly complex and requires specialized facilities, which increases costs and limits the availability of this life-saving therapy. Recently, interest in *in vivo* CAR-T cell generation using LV has intensified to alleviate many bottlenecks presently associated with *ex vivo* transduction.[40–43] Although we did not characterize the immunogenicity of SJ293TS-DPB-derived viral particles in this study, we did confirm that these viral particles are devoid of B2M and MHC-I and may be less immunogenic than B2M containing LV.

This report describes the development of a genetically modified 293T cell line, SJ293TS-DPB, designed to support the manufacturing of both sense and anti-sense clinical grade LVs and be grown in suspension using SFM. In addition, the absence of B2M better positions the SJ293TS-DPB cell line to support future needs of LV-based cell and gene therapies. We have shown that LVs derived from this process can efficiently transduce cells commonly targeted in human gene and cell therapy. Our production scheme is simple to employ, robust, and is suitable for cGMP manufacturing. Currently, we are preparing to establish a master cell bank for use in our GMP facility.

MATERIALS AND METHODS

Cell lines

SJ293TS cells, described in Bauler et al., and SJ293TS-DPB cells were maintained in Freestyle 293 Expression media (Thermo Fisher Scientific, Waltham, MA), except when LV-MAX production media (Thermo Fisher Scientific) was used as noted in the text, at 37°C with 8% CO_2 and shaking at 125 RPM with an orbital diameter of 25 mM.[13] To avoid foam generation when cells were grown in a 5-L flask with culture volumes of 0.5–1 L, shaking was reduced to 90 RPM. HOS-6A5 cells, derived from ATCC CLR-1543, were maintained in Dulbecco's modified Eagle's medium (Corning, Corning, NY) supplemented with 10% fetal bovine serum (FBS) (Seradigm, Radnor, PA) and 2 mM L-alanyl-L-glutamine (Corning) (D10) at 37°C with 5% CO_2. This cell line contains four copies of a fourth-generation lentiviral vector, lacking an HIV *psi* packaging signal, expressing the murine CAT1 gene. All cell lines were split every 2 to 3 days.

Plasmids

All vector plasmids were made using standard molecular biology techniques and sequenced in full. pSJL12-MND-GFP-AF and pSJL21-MND-GFP-AF express the GFP reporter under control of the MND promoter in either the forward or reverse orientation,

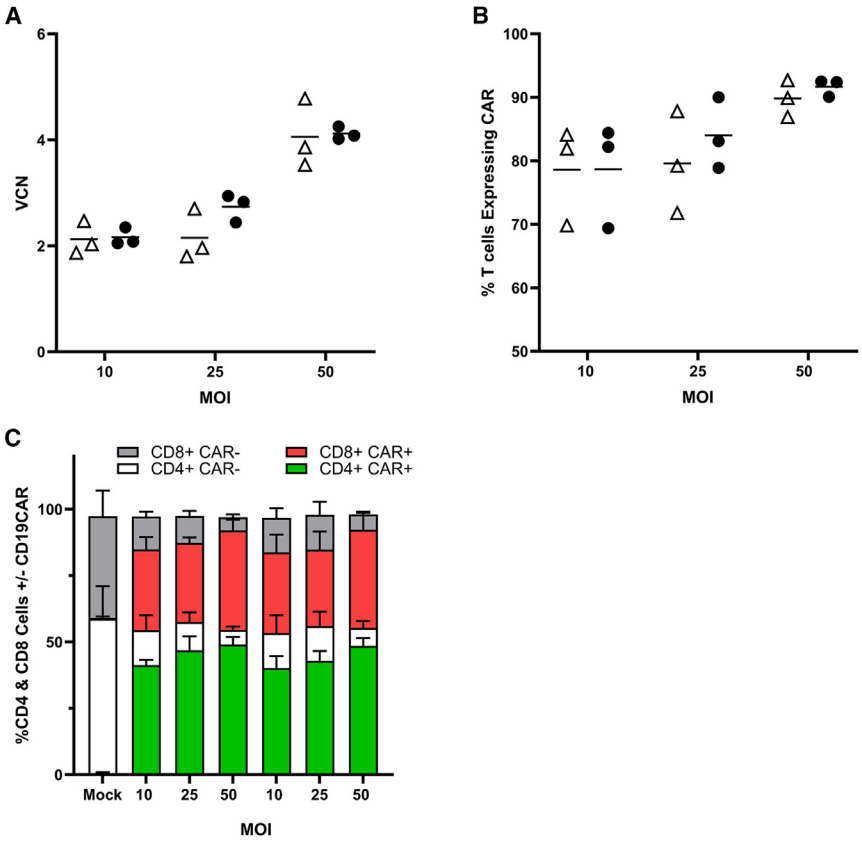

Figure 6. Analysis of human donor T cells transduced with the lentiviral vector, SJL643

T cells from three healthy human donors were transduced with the lentiviral vector, SJL643, using an MOI of 10, 25, or 50 produced from either SJ293TS (Δ) or SJ293TS-DPB (●). (A) T cell vector copy number (VCN). (B) Percentage of CAR-expressing T cells. (C) Ratio of $CD4^+$ $CAR^{\pm}$ and $CD8^+$ $CAR^{\pm}$ T cells. For (A) and (B), each data point represents a single donor with the mean represented by a bar. All analyses were performed 7 days post-transduction.

respectively. pSJL643-AF expresses CD20 and an anti-CD123 CAR using a 2A peptide sequence from *Thosea asigna* virus (T2A).[44] pSJL651 expresses the 41BB ligand followed by an anti-B7H3 CAR via a P2A peptide sequence.[45] pCL40i4r-EF1a-hgcOPT expresses a codon-optimized human common gamma chain.[14] Plasmids with the "AF" designation were selected using antibiotic-free selection cassette, RNA-OUT, from Aldeveron as described in Bauler et al.[13] Sequence files for all plasmids used in this study are available upon request.

Lentiviral vector production

LV production was performed as described in Bauler et al.[13] Briefly, cells at a density of 2×10^6 cells per mL, or as stated in the text, were transfected with a vector plasmid and the following helper plasmids, pCAG-kGP1-1R-AF (*gagpol*), pCAG-VSVG-AF (VSV-G), and pCMV-REV-AF (Rev), at a ratio of 14:4:2:0.25, respectively. All transfections were performed using PEIpro (Polyplus Transfection, Strasbourg, France). Transfection reagents were scaled up proportionally depending on the volume of vector production. Before mixing, plasmid DNA was diluted in phosphate-buffered saline (PBS) (Corning) to 40 μg/mL, and PEIpro was diluted to 80 μg/mL in PBS. The transfection mixture was then incubated for approximately 5 min before being added directly to the cell culture. Vector preparations scheduled for downstream purification or as noted in the text were diluted with an equal volume of fresh Freestyle 293 Expression media. At the same time, Benzonase was added to the cell culture to achieve a final concentration of 6.25 U/mL. Vector supernatants were harvested 48 h post transfection and clarified by centrifugation to remove cells, filtered through 0.45- and 0.22-μm filters and either subjected to further purification or stored at −80°C before titration.

For downstream processing, LV containing supernatant was adjusted to 300 mM NaCl with 50 mM Tris pH, 8.0 before being loaded onto either a 0.86 mL Mustang Q XT Acrodisc or a 5 mL Mustang Q XT5 ion-exchange capsule (Cytiva, Marlborough, MA) per the manufacturer's instructions using an Akta Avant chromatography system (Cytiva). The Mustang Q XT Acrodisc was used when the total LV supernatant volume was $\leq$100 mL. For larger volumes, the 5-mL Mustang Q XT5 ion-exchange capsule was employed. Regardless of column used, after loading, the membrane was washed with 10 column volumes of 300 mM NaCl with 50 mM Tris pH, 8.0, and LV particles were eluted from the column by using 2 M NaCl, 50 mM Tris pH, 8.0. When using the Mustang Q XT Acrodisc, viral particles were eluted in 1 mL and directly loaded into a PD10 desalting column (Cytiva). After buffer exchange, the eluate was mixed 1:1 with X-VIVO 10 or X-VIVO 15 media (Lonza) for a final volume of 2 mL. Eluates from the 5-mL Mustang Q XT5 ion-exchange capsule were diluted 5-fold with PBS and diafiltrated twice in PBS using a Vivaflow 50 with a 100,000 molecular weight cutoff (Sartorius AG, Goettingen, Germany) according to the manufacturer's instructions before a final diafiltration was performed in X-VIVO 10 or X-VIVO 15 media (Lonza) to achieve a final concentration of about 50-fold from the starting material. Purified and concentrated vectors were then 0.22-μm filtered, aliquoted, and stored at −80°C before being titrated.

Cas9-VLP production

Cas9-VLPs were produced similarly to LVs as described above by transfection of 20 mL SJ293TS cells using 18 μg of pCAGG-HIVgpco-Cas9co, 8 μg of sgRNA-expressing constructs, 2 μg of pCAG-VSVG-AF, and 0.25 μg of pCMV-Rev-AF. pCAGG-HIVgpco-Cas9co expresses a codon-optimized HIV *gagpol* and

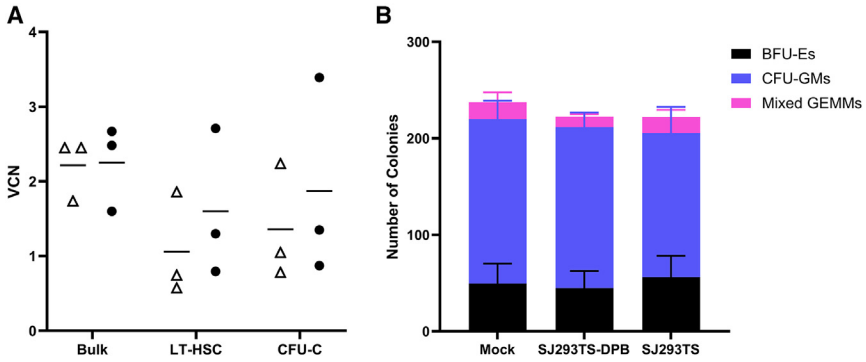

Figure 7. CD34⁺ HSC transduction with CL40i4r-EF1a-hgcOPT

CD34⁺ HSC from three healthy human donors were transduced with the lentiviral vector, CL40i4r-EF1a-hgcOPT, with an MOI of 50 produced from either SJ293TS (Δ) or SJ293TS-DPB (●). (A) VCN was determined for bulk cells, LT-HSC, and pooled CFU-C 7 days, 4 days, and 12 days post-transduction, respectively. Each data point represents a single donor, and the mean is represented by the bar. (B) Number of BFU-E, CFU-GM, or mixed GEMM colonies growing in MethoCult after 12 days.

Cas9. sgRNAs directed against the target of interest (Table S1) were designed and cloned in a proprietary plasmid backbone (unpublished data, plasmids sequence available upon request) to express in SJ293TS cells under the U6 promoter efficiently. Twenty-four hours post-transfection, Benzonase was added to a final concentration of 6.25 U/mL, and 48 h post-transfection, the supernatant was collected and clarified by centrifugation at 330 × *g*. The supernatant was 0.22-μm filtered and stored at −80°C before being used.

Targeted deep sequencing

A total of 100,000 cells were collected by centrifugation at 330 × *g*. After removing the supernatant, cells were lysed with 10 μL of 10 mM Tris pH 8.0, 2 mM EDTA pH 8.0, 0.2% Triton X-100, 200 μg/mL proteinase K, and incubated for 6 min at 65°C and 2 min at 98°C. This PCR-ready genomic DNA was subjected to targeted deep sequencing by NGS followed by analysis with CRIS.py by the Center for Advanced Genome Engineering at St Jude Children's Research Hospital. Briefly, primers reported in Table S4 were used to amplify the four loci targeted by Cas9-VLP. To evaluate large deletions and obtain amplicon amenable to NGS, primers CAGE1167.PKR.F and CAGE1168.PKR.R and primers CAGE1169.B2M.F and CAGE1170.B2M.R were used for PKR and B2M, respectively. A second PCR was used to add appropriate Illumina indexes. The resulting amplicons were subjected to 250-bp paired-end sequencing using the MiSeq System (Illumina, San Diego, CA).

Protein extraction and western blot analysis

Protein samples were prepared by incubation of cell pellets with radioimmunoprecipitation assay (RIPA) Lysis and Extraction Buffer and HALT Protease Inhibitor Cocktail (Thermo Fisher Scientific) on ice for 30 min. Lysates were then cleared through centrifugation at 4°C and 10,000 × *g* for 15 min, and supernatants were collected and used for a Pierce BCA Protein Assay (Thermo Fisher Scientific) to determine protein concentration. Total protein (40 μg per lane) was resolved on 4%–15% Mini-PROTEAN TGX gels (Bio-Rad, Carlsbad, CA), and then transferred to an Immobilon-FL PVDF membrane using wet transfer for 30 min at 100 V constant voltage.

For protein isolation from lentiviral particles, viral supernatants were subjected to ultracentrifugation at 100,000 × *g* for 90 min. Cleared supernatant was removed, and viral pellets were suspended in PBS and incubated on ice for 2 h. An equal volume of RIPA buffer (described above) was added to the suspended viral particles and processed as described above. Total protein (30 μg for B2M detection or 100 ng for HIV1 p24 detection) was used for downstream protein gel electrophoresis and blotting.

The primary antibodies used were rabbit anti-PKR (Cell Signaling, Danvers, MA, #12297; clone D7F7), rabbit anti-B2M (Cell Signaling, #12851; clone D8P1H), mouse anti-Gapdh (Santa Cruz Biotechnology, Dallas, TX, sc-47724; clone 0411), and mouse anti-HIV1 p24 (Invitrogen, Thermo-Fischer Scientific, MA, 1–71515; clone 5). Blocking was performed in TBS-based Intercept Blocking Buffer (LI-COR Biotechnology, Lincoln, NE) with 0.1% Tween 20 (Bio-Rad) added during primary and secondary antibody incubations. The secondary antibodies used were goat anti-rabbit IRDye 800CW and goat anti-mouse IRDye 680LT (LI-COR Biotechnology, #926–32211 and #926–68020). Membranes were imaged using an LI-COR Odyssey M Infrared Imaging System.

The Jess Automated Western Blot system (Bio-Techne, Minneapolis, MN) was used according to the manufacturer's instructions for the MHC-I western blot. Briefly, 3 μg of viral lysates in RIPA buffer were prepared with the EZ standard Fluorescent Master mix containing 200 mM dithiothreitol solution and loaded on a 12- to 230-kDa cartridge (Bio-Techne). EZ biotinylated ladder was used together with the streptavidin-NIR ready-made solution. Antibody diluent 2 was used during blocking and to prepare the solutions for primary and secondary antibody incubations. For detection, a 1:150 dilution of HLA class I ABC rabbit Polyclonal antibody (15240-1-AP, Proteintech, Rosemont, IL) and a 1:250 dilution of HIV-1 Gag p24 mouse antibody Clone # 749122 (Bio-Techne) were used to detect MHC-I and HIV-1 p24, respectively. The Anti-Rabbit HRP Conjugate (Bio-Techne) and the Anti-Mouse Secondary NIR Antibody (Bio-Techne) were used as secondary antibodies at 1:20 dilution.

HIV-1 p24 ELISA

HIV-1 p24 determination was performed using the Lumit p24 Immunoassay (Promega, Madison, WI) according to the manufacturer's instructions.

LV titer and copy number determination

To determine viral titers, we used the same method as described previously in Bauler et al.[13] Briefly, HOS-6A5 cells were seeded at a density of 1×10^5 cells per well of a 6-well plate or 1.6×10^4 cells per well of a 96-well dish 2 h before transduction. Vector aliquots were thawed at room temperature, serially diluted, and added to HOS-6A5 cells in the presence of Polybrene (5–8 μg/mL, MilliporeSigma, Burlington, MA) in a total volume of either 1 mL or 200 mL depending on size of well. The next day, the media was exchanged. Transduced HOS-6A5 cells were harvested 4 days post-transduction. Titers for GFP-expressing LVs were determined by flow cytometry using an Attune NxT flow cytometer (Thermo Fisher Scientific) using the following formula: percent of GFP^+ cells divided by number of cells seeded multiplied by the dilution factor = TU/mL. Alternatively, HOS-6A5 cell titer and VCN in transduced primary human T cells and $CD34^+$ cells was determined by droplet digital PCR (ddPCR) as follows: Genomic DNA was isolated from transduced cells as described above for targeted deep sequencing. The genomic DNA was then digested with *Msp*I and used as a template in PCR by using a ddPCR instrument (QX200 Bio-Rad). The following primer-probe sets were used to amplify the HIV *psi* sequence and the endogenous control gene, *RPP30*, 5′-ACTTGAAAGCGAAAGGGAAAC-3′, 5′-CACCCATCTCTCTCCTTCTAGCC-3′ and probe 5′-56-FAM-AGCTCTCTC-ZEN-GACGCAGGACTCGGC-3IABkFQ-3′ and 5′-GCGGCTGTCTCCACAAGT-3′, 5′-GATTTGGACCTGCGAGCG-3′ and probe 5′-5HEX-CTGACCTGA-ZEN-AGGCTCT-3IABkFQ-3′, respectively. Vector titers and copy number were determined by calculating the number of copies of HIV *psi* to every two copies of *RPP30*, multiplied by the number of cells transduced, and if necessary, multiplied by the dilution factor.

T cell transduction

Healthy donor-derived human peripheral blood apheresis cells were purchased from StemExpress (Folsom, CA). The cells were labeled with anti-CD4/CD8 microbeads and $CD4^+/CD8^+$ T cells were purified by using the CliniMACS system (Miltenyi Biotec, Bergisch Gladbach, Germany). $CD4^+$ and $CD8^+$ T cells from peripheral blood mononuclear cells were suspended in X-VIVO 15 media with 5% human AB serum (Valley Biomedicals, Inc., Winchester, VA) and 10 ng/mL of recombinant human interleukin (IL)-7 and IL-15 (Miltenyi Biotec) (X-VIVO 15-5% HSA/IL7/IL15, hereafter). Then, cells were activated upon incubation at 37°C with 5% CO_2 for 24 h on anti-CD3 and anti-CD28 antibody (Miltenyi Biotec) coated 12-well plate (Corning) for a final concentration of 2 μg/mL each. The activated T cells were washed and suspended in X-VIVO 15-5% HSA/IL7/IL15, followed by transduction with two anti-CD123 chimeric antigen receptor-expressing vectors at an MOI of 10, 25, and 50 in a total volume of 100 μL. Twenty-two hours post-transduction, the cells were washed and maintained in X-VIVO 15%–5% HSA/IL7/IL15.

$hCD34^+$ HSC transduction and CFU-c assay

The St Jude Human Applications Laboratory purified $CD34^+$ cells from granulocyte-colony stimulating factor mobilized peripheral blood of healthy volunteers purchased via Charles River Laboratory (Wilmington, MA) or StemExpress (Folsom, CA). $CD34^+$ cells were cultured in X-VIVO-10 (Lonza, Walkersville, MD) with 100 ng/mL of stem cell factor (SCF), Fms-related tyrosine kinase 3 ligand (FLT3-ligand), thrombopoietin (TPO) (CellGenix, Freiburg, Germany), and 2 mM L-alanyl-L-glutamine (Corning). Cells were primed overnight in media at a density of 1×10^6 cells/mL and seeded at a density of 2×10^6 cells/mL in wells of a 12-well plate (1 mL final) and transduced with vector at an MOI of 50 in the presence of 8 mg/mL protamine sulfate (Fresenius Kabi, Lake Zurich, IL), 1% recombinant human serum albumin (Grifols Biologics, Los Angeles, CA), and 100 ng/mL SCF, FLT3, and TPO. Twenty-four hours post transduction, cells were collected by centrifugation and suspended in fresh culture media to be either maintained in liquid culture (4 days for sort or 7 days for VCN), or to seed 1,800 cells in MethoCult H4434 Classic (Stemcell Technologies, Vancouver, Canda) for maintenance in STEMVision 6-well plates (Stemcell Technologies) at 37°C with CO_2 for 12 days. CFU-Cs were analyzed using STEMvision's automated CFU assay reader and software (Stemcell Technologies), prior to being pooled for VCN analyses.

$hCD34^+$ HSC staining and sorting

Four days post transduction, 5 to 10 million $CD34^+$ cells were stained with the following antibodies: hCD34-FITC (BioLegend, San Diego, CA; Cat #353504), hCD38-PE (BioLegend; Cat #356604), hCD90-APC (BioLegend; Cat #328114), hCD45RA-BV650 (BD Biosciences, San Jose, CA; Cat# 563963). Live/dead cell marker was NucBlue Fixed Cell ReadyProbes reagent (DAPI) (ThermoFisher Scientific). The gating strategy used to sort $CD34^+CD38^-CD90^+CD45RA^-$ (LT-HSC) cells was as follows: viable ($DAPI^-$) singlets (FSC-A/SSC-W) were gated on $CD34^+CD38^-$ cells ($CD38^-$PE-A vs. $CD34^+$FITC-A), and this population was sorted into $CD45RA^-$BV650 FL13-A and $CD90^+$APC-A cells.

Flow cytometry

A four-laser (Blue/red/yellow/violet) Attune NxT Flow cytometer (Thermo Fisher Scientific) instrument was used to acquire flow cytometry data. FlowJo v.10 (FlowJo, Ashland, OR) was used for data analysis and graphic representation. Genetically modified anti-CD123 chimeric antigen receptor-expressing T cells were detected by G4S Linker (E7O2V) Rabbit mAb (Alexa Fluor 647 Conjugate, Cell Signaling Technology, Danvers, MA). Brilliant Violet 711 anti-human CD4 Antibody clone SK3 (BioLegend) and BD Horizon BV510 Mouse Anti-Human CD8 Clone SK1 (BD Biosciences) were used to differentiate T cell subtypes. SJ293TS and derived clones were stained with BD Pharmingen PE Mouse Anti-Human β2-Microglobulin clone TÜ99 (BD Biosciences) or with BD Pharmingen PE Mouse Anti-Human HLA-ABC clone W6/32 (BD Biosciences). The cells were incubated for 30 min at 4°C in the dark in the presence of the antibody mixture and washed with MACS Running Buffer before being suspended in it for analysis. NucBlue Fixed Cell ReadyProbes Reagent (DAPI -Thermo Fisher Scientific) was added to distinguish live cells from dead cells before analysis.

Statistical analyses

One way or two-way analysis of variance (ANOVA) tests are used to compare the effect of different lentiviral vectors or time to transfection. Pairwise t test with Bonferroni correction is used to test between-group difference in titer average or transfection efficiency. Shapiro-Wilks's test as well as visual inspection of the QQ plots are used to test for the normality assumption, and Bartlett's test is used to test for the homoscedasticity assumption for the ANOVA tests. If either assumption is found to be violated, a Wilcoxon Rank-sum test is performed instead of a t test, a Kruskal-Wallis test is used instead of a one-way ANOVA to compare two or more groups, or a log transformation of the data is used for the two-way ANOVA tests to compare the effect of two or more factors and/or their interaction. All statistical tests and conclusions are drawn using the standard 5% significance level with multiple testing corrections applied as appropriate. All analyses were performed using R software (R Foundation for Statistical Computing, 4.3.1) on an 11th Gen Intel(R) Core (TM) i7-1185G7 processor.

DATA AND CODE AVAILABILITY

The data that support the findings reported in this study are available upon request to the corresponding author.

SUPPLEMENTAL INFORMATION

Supplemental information can be found online at https://doi.org/10.1016/j.omtm.2024.101270.

ACKNOWLEDGMENTS

This study was supported with funding from the American Lebanese Syrian Associated Charities. S.N. and C.L. were in part supported by National Institutes of Health/National Cancer Institute grant (P30 CA021765). Graphical abstract created with BioRender.com.

AUTHOR CONTRIBUTIONS

M.B., B.L., J.B., C.W., F.F., M.M.W., J.P., N.S., D.L., and S.Z. developed methods, performed experiments, and analyzed data. S.N. and C.L. performed statistical analyses. R.E.T. conceived experiments, interpreted data, and wrote the manuscript. All authors read and approved the final manuscript.

DECLARATION OF INTERESTS

The authors declare no competing interests.

REFERENCES

1. Sakuma, T., Barry, M.A., and Ikeda, Y. (2012). Lentiviral vectors: basic to translational. Biochem. J. *443*, 603–618.
2. Ghaleh, H.E.G., Bolandian, M., Dorostkar, R., Jafari, A., and Pour, M.F. (2020). Concise review on optimized methods in production and transduction of lentiviral vectors in order to facilitate immunotherapy and gene therapy. Biomed. Pharmacother. *128*, 110276.
3. Milone, M.C., and O'Doherty, U. (2018). Clinical use of lentiviral vectors. Leukemia *32*, 1529–1541.
4. Perry, C., and Rayat, A.C.M.E. (2021). Lentiviral Vector Bioprocessing. Viruses *13*, 268.
5. Naldini, L., Blömer, U., Gallay, P., Ory, D., Mulligan, R., Gage, F.H., Verma, I.M., and Trono, D. (1996). In vivo gene delivery and stable transduction of nondividing cells by a lentiviral vector. Science *272*, 263–267.
6. Kumar, M., Keller, B., Makalou, N., and Sutton, R.E. (2001). Systematic determination of the packaging limit of lentiviral vectors. Hum. Gene Ther. *12*, 1893–1905.
7. Cattoglio, C., Facchini, G., Sartori, D., Antonelli, A., Miccio, A., Cassani, B., Schmidt, M., von Kalle, C., Howe, S., Thrasher, A.J., et al. (2007). Hot spots of retroviral integration in human CD34+ hematopoietic cells. Blood *110*, 1770–1778.
8. (2023). FDA Approves First Gene Therapies to Treat Patients with Sickle Cell Disease. FDA. https://www.fda.gov/news-events/press-announcements/fda-approves-first-gene-therapies-treat-patients-sickle-cell-disease.
9. Chancellor, D., Barrett, D., Nguyen-Jatkoe, L., Millington, S., and Eckhardt, F. (2023). The state of cell and gene therapy in 2023. Mol. Ther. *31*, 3376–3388.
10. (2019). Statement from FDA Commissioner Scott Gottlieb, M.D. and Peter Marks, M.D., Ph.D., Director of the Center for Biologics Evaluation and Research on new policies to advance development of safe and effective cell and gene therapies. FDA. https://www.fda.gov/news-events/press-announcements/statement-fda-commissioner-scott-gottlieb-md-and-peter-marks-md-phd-director-center-biologics.
11. Martínez-Molina, E., Chocarro-Wrona, C., Martínez-Moreno, D., Marchal, J.A., and Boulaiz, H. (2020). Large-Scale Production of Lentiviral Vectors: Current Perspectives and Challenges. Pharmaceutics *12*, 1051.
12. Powers, A.D., Drury, J.E., Hoehamer, C.F., Lockey, T.D., and Meagher, M.M. (2020). Lentiviral Vector Production from a Stable Packaging Cell Line Using a Packed Bed Bioreactor. Mol. Ther. Methods Clin. Dev. *19*, 1–13.
13. Bauler, M., Roberts, J.K., Wu, C.C., Fan, B., Ferrara, F., Yip, B.H., Diao, S., Kim, Y.I., Moore, J., Zhou, S., et al. (2020). Production of Lentiviral Vectors Using Suspension Cells Grown in Serum-free Media. Mol. Ther. Methods Clin. Dev. *17*, 58–68.
14. Throm, R.E., Ouma, A.A., Zhou, S., Chandrasekaran, A., Lockey, T., Greene, M., De Ravin, S.S., Moayeri, M., Malech, H.L., Sorrentino, B.P., and Gray, J.T. (2009). Efficient construction of producer cell lines for a SIN lentiviral vector for SCID-X1 gene therapy by concatemeric array transfection. Blood *113*, 5104–5110.
15. Tomás, H.A., Rodrigues, A.F., Carrondo, M.J.T., and Coroadinha, A.S. (2018). LentiPro26: novel stable cell lines for constitutive lentiviral vector production. Sci. Rep. *8*, 5271.
16. Tona, R.M., Shah, R., Middaugh, K., Steve, J., Marques, J., Roszell, B.R., and Jung, C. (2023). Process intensification for lentiviral vector manufacturing using tangential flow depth filtration. Mol. Ther. Methods Clin. Dev. *29*, 93–107.
17. Tang, Q.L., Gu, L.X., Xu, Y., Liao, X.H., Zhou, Y., and Zhang, T.C. (2021). Establishing functional lentiviral vector production in a stirred bioreactor for CAR-T cell therapy. Bioengineered *12*, 2095–2105.
18. Tran, M.Y., and Kamen, A.A. (2022). Production of Lentiviral Vectors Using a HEK-293 Producer Cell Line and Advanced Perfusion Processing. Front. Bioeng. Biotechnol. *10*, 887716.
19. Zufferey, R., Dull, T., Mandel, R.J., Bukovsky, A., Quiroz, D., Naldini, L., and Trono, D. (1998). Self-inactivating lentivirus vector for safe and efficient *in vivo* gene delivery. J. Virol. *72*, 9873–9880.
20. Han, J., Tam, K., Ma, F., Tam, C., Aleshe, B., Wang, X., Quintos, J.P., Morselli, M., Pellegrini, M., Hollis, R.P., and Kohn, D.B. (2021). β-Globin Lentiviral Vectors Have Reduced Titers due to Incomplete Vector RNA Genomes and Lowered Virion Production. Stem Cell Rep. *16*, 198–211.
21. Breda, L., Ghiaccio, V., Tanaka, N., Jarocha, D., Ikawa, Y., Abdulmalik, O., Dong, A., Casu, C., Raabe, T.D., Shan, X., et al. (2021). Lentiviral vector ALS20 yields high hemoglobin levels with low genomic integrations for treatment of beta-globinopathies. Mol. Ther. *29*, 1625–1638.
22. Arumugam, P.I., Scholes, J., Perelman, N., Xia, P., Yee, J.K., and Malik, P. (2007). Improved human β-globin expression from self-inactivating lentiviral vectors carrying the chicken hypersensitive site-4 (cHS4) insulator element. Mol. Ther. *15*, 1863–1871.
23. Negre, O., Bartholomae, C., Beuzard, Y., Cavazzana, M., Christiansen, L., Courne, C., Deichmann, A., Denaro, M., de Dreuzy, E., Finer, M., et al. (2015). Preclinical Evaluation of Efficacy and Safety of an Improved Lentiviral Vector for the Treatment of β-Thalassemia and Sickle Cell Disease. Curr. Gene Ther. *15*, 64–81.

24. Amendola, M., Venneri, M.A., Biffi, A., Vigna, E., and Naldini, L. (2005). Coordinate dual-gene transgenesis by lentiviral vectors carrying synthetic bidirectional promoters. Nat. Biotechnol. *23*, 108–116.

25. Tian, J., and Andreadis, S.T. (2009). Independent and high-level dual-gene expression in adult stem-progenitor cells from a single lentiviral vector. Gene Ther. *16*, 874–884.

26. Hu, P., Bi, Y., Ma, H., Suwanmanee, T., Zeithaml, B., Fry, N.J., Kohn, D.B., and Kafri, T. (2018). Superior lentiviral vectors designed for BSL-0 environment abolish vector mobilization. Gene Ther. *25*, 454–472.

27. Chen, Y.G., and Hur, S. (2022). Cellular origins of dsRNA, their recognition and consequences. Nat. Rev. Mol. Cell Biol. *23*, 286–301.

28. Gantier, M.P., and Williams, B.R.G. (2007). The response of mammalian cells to double-stranded RNA. Cytokine Growth Factor Rev. *18*, 363–371.

29. Piras, F., and Kajaste-Rudnitski, A. (2021). Antiviral immunity and nucleic acid sensing in haematopoietic stem cell gene engineering. Gene Ther. *28*, 16–28.

30. Pernod, G., Fish, R., Liu, J.W., and Kruithof, E.K. (2004). Increasing lentiviral vector titer using inhibitors of protein kinase R. Biotechniques *36*, 576–580.

31. Ferreira, C.B., Sumner, R.P., Rodriguez-Plata, M.T., Rasaiyaah, J., Milne, R.S., Thrasher, A.J., Qasim, W., and Towers, G.J. (2020). Lentiviral Vector Production Titer Is Not Limited in HEK293T by Induced Intracellular Innate Immunity. Mol. Ther. Methods Clin. Dev. *17*, 209–219.

32. Han, J., Tam, K., Tam, C., Hollis, R.P., and Kohn, D.B. (2021). Improved lentiviral vector titers from a multi-gene knockout packaging line. Mol. Ther. Oncolytics *23*, 582–592.

33. Milani, M., Annoni, A., Bartolaccini, S., Biffi, M., Russo, F., Di Tomaso, T., Raimondi, A., Lengler, J., Holmes, M.C., Scheiflinger, F., et al. (2017). Genome editing for scalable production of alloantigen-free lentiviral vectors for *in vivo* gene therapy. EMBO Mol. Med. *9*, 1558–1573.

34. Bushman, F.D. (2020). Retroviral Insertional Mutagenesis in Humans: Evidence for Four Genetic Mechanisms Promoting Expansion of Cell Clones. Mol. Ther. *28*, 352–356.

35. Bagchi, D.N., and Iyer, V.R. (2016). The Determinants of Directionality in Transcriptional Initiation. Trends Genet. *32*, 322–333.

36. Gatignol, A. (2014). PKR and HIV Replication. In Encyclopedia of AIDS, T.J. Hope, M. Stevenson, and D. Richman, eds. (Springer New York), pp. 1–6.

37. Bannwarth, S., and Gatignol, A. (2005). HIV-1 TAR RNA: The target of molecular interactions between the virus and its host. Curr. HIV Res. *3*, 61–71.

38. Bou-Nader, C., Gordon, J.M., Henderson, F.E., and Zhang, J. (2019). The search for a PKR code-differential regulation of protein kinase R activity by diverse RNA and protein regulators. RNA *25*, 539–556.

39. Dzananovic, E., Patel, T.R., Deo, S., McEleney, K., Stetefeld, J., and McKenna, S.A. (2013). Recognition of viral RNA stem-loops by the tandem double-stranded RNA binding domains of PKR. RNA *19*, 333–344.

40. Michels, A., Ho, N., and Buchholz, C.J. (2022). Precision medicine: In vivo CAR therapy as a showcase for receptor-targeted vector platforms. Mol. Ther. *30*, 2401–2415.

41. Michels, K.R., Sheih, A., Hernandez, S.A., Brandes, A.H., Parrilla, D., Irwin, B., Perez, A.M., Ting, H.A., Nicolai, C.J., Gervascio, T., et al. (2023). Preclinical proof of concept for VivoVec, a lentiviral-based platform for *in vivo* CAR T-cell engineering. J. Immunother. Cancer *11*, e006292.

42. Wakao, R., and Fukaya-Shiba, A. (2023). In vivo CAR T cells and targeted gene delivery: A theme for the Pharmaceuticals and Medical Devices Agency Science Board to address. Front. Med. *10*, 1141880.

43. Xin, T., Cheng, L., Zhou, C., Zhao, Y., Hu, Z., and Wu, X. (2022). In-Vivo Induced CAR-T Cell for the Potential Breakthrough to Overcome the Barriers of Current CAR-T Cell Therapy. Front. Oncol. *12*, 809754.

44. Riberdy, J.M., Zhou, S., Zheng, F., Kim, Y.I., Moore, J., Vaidya, A., Throm, R.E., Sykes, A., Sahr, N., Bonifant, C.L., et al. (2020). The Art and Science of Selecting a CD123-Specific Chimeric Antigen Receptor for Clinical Testing. Mol. Ther. Methods Clin. Dev. *18*, 571–581.

45. Nguyen, P., Okeke, E., Clay, M., Haydar, D., Justice, J., O'Reilly, C., Pruett-Miller, S., Papizan, J., Moore, J., Zhou, S., et al. (2020). Route of 41BB/41BBL Costimulation Determines Effector Function of B7-H3-CAR.CD28ζ T Cells. Mol. Ther. Oncolytics *18*, 202–214.